

# Wideband Balun Bandpass Filter Based on a Balanced Circuit

Li Sheng Yang<sup>1</sup> and Wenjie Feng<sup>2, \*</sup>

**Abstract**—A novel wideband balun filter based on a symmetric four-port balanced circuit is proposed in this paper. A pair of open coupled lines is used to realize DC suppression and in-band balance improvement for the balun bandpass filter. The bandwidth can be easily adjusted by changing the characteristic impedance of transmission lines in the balanced circuit. For the proposed balun bandpass filter, excellent in-band balance performance (amplitude and phase imbalance are less than 0.25 dB and 1.3° respectively) over the passband are achieved. A wideband balun bandpass filter prototype with center frequency 3.75 GHz and 3-dB bandwidth 33.8% is designed and fabricated. Good agreement can be observed between the measured results and theoretical expectations.

## 1. INTRODUCTION

As one of the most important RF front-end functional passive devices, the balun bandpass filter integrating balun and bandpass filter is a necessary component for converting a balanced signal into an unbalanced one for a specified bandpass characteristic. In the past few years, several techniques have been proposed to design narrow/dual-band and wideband balun bandpass filters [1–5]. Both characteristics of balun and bandpass filter can be easily realized in these filter structures. However, the application of these filters is limited for their in-band balun performances are not convenient to optimize.

Recently, several symmetric four-port balanced filter structures have been developed to build balun filters with one of the ports opened [6–8]. By using the mixed mode  $S$ -parameters theoretical analysis [9] and feasible solutions [10], a three-port balun bandpass filter with desired bandpass response such as controllable fractional bandwidth, good selectivity, and extended stopband can be realized. In addition, due to the possibility of minimizing the common-mode noise in the symmetric four-port balanced bandpass filter, the in-band balun performance of the three-port balun bandpass filter can be further optimized [6–8]. However, multilayer coupling technology is needed to realize wider bandwidth for the three-port balun bandpass filter, which increases the fabrication difficulty [6].

In this work, a novel wideband three-port balun bandpass filter is proposed based on the balanced circuit in [11, 12] a pair of open coupled lines is used to realize DC suppression and improve the in-band balance for the balun filter. A high-order passband with high selectivity and extended stopband for the wideband balun bandpass filter can be achieved. All the structures are simulated with Ansoft HFSS v.11.0 and constructed on a dielectric substrate with  $\epsilon_r = 2.65$ ,  $h = 0.5$  mm and  $\tan \delta = 0.003$ .

## 2. DESIGN OF THE PROPOSED WIDEBAND BALUN BANDPASS FILTER

### 2.1. Basic Theoretical Analysis

Figure 1 shows a three-port balun filter based on a symmetric four-port balanced filter. The  $S$ -matrix of the three-port balun can be extracted from the differential/common -mode theoretical analysis as

---

Received 15 August 2014, Accepted 15 September 2014, Scheduled 6 October 2014

\* Corresponding author: Wenjie Feng (fengwenjie1985@163.com).

<sup>1</sup> Department of Electronics and Information Technique, Zhengde Polytechnic College, Nanjing 211106, China. <sup>2</sup> Department of Communication Engineering, Nanjing University of Science & Technology, Nanjing 210094, China.

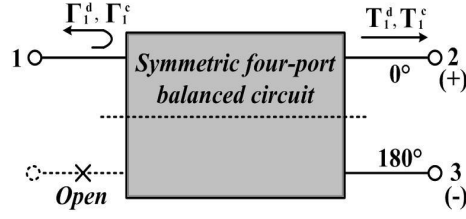


**Figure 1.** Schematic of a three-port balun filter based on balanced circuit.

follows [4, 9]:

$$S_{11} = (\Gamma_1^d + \Gamma_1^c - 2\Gamma_1^d\Gamma_1^c) / (2 - \Gamma_1^d - \Gamma_1^c) \quad (1)$$

$$S_{21} = -S_{31} = T_1^d(1 - \Gamma_1^c) / (2 - \Gamma_1^d - \Gamma_1^c) \quad (2)$$

For a well-balanced balun structure, an equal power division with  $180^\circ$  phase difference should be realized between ports 2 and 3 ( $S_{21} = -S_{31}$ ). In addition, to achieve a wide bandwidth and good amplitude balance,  $S_{11}$  should equal to zero, and a feasible solution for differential/common-mode reflection and transmission coefficients for the three-port balun can be obtained as [4, 9]:

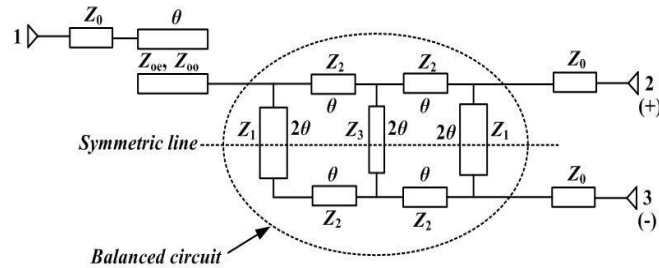
$$\Gamma_1^d = 1/3, \quad \Gamma_1^c = -1 \quad (3)$$

$$T_1^d = -2j\sqrt{2}/3, \quad T_1^c = 0 \quad (4)$$

Above Equations (3) and (4) describe the requirements on the three-port balun filter, which is actually transformed from the symmetric four-port balanced filter structure with one of the ports opened. In addition, to realize good input impedance matching at the unbalanced port (port 1), the common-mode input impedance should be twice the input termination impedance [6, 10]. For such purpose, a pair of open coupled lines is used to match the input impedance, and the in-band balun performance of the proposed three-port balun bandpass filter also can be optimized.

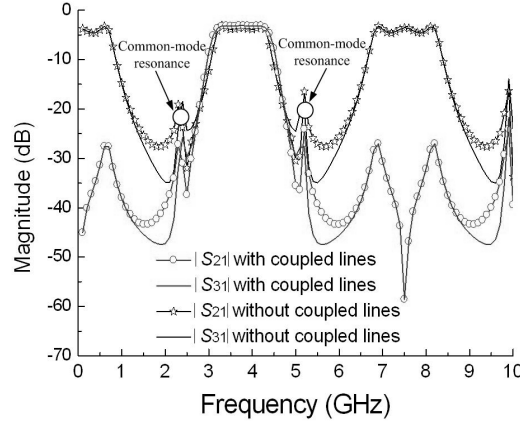
## 2.2. Proposed Wideband Balun Bandpass Filter

Figure 2 illustrates the ideal circuit of the proposed wideband balun bandpass filter. A two-stage four-port balanced circuit in [10] with one port opened is located in the center of the balun bandpass filter. A pair of open coupled lines (even/odd-mode characteristic impedance  $Z_{oe}$  and  $Z_{oo}$ ) is connected to the unbalanced port, and three microstrip lines with characteristic impedance  $Z_0 = 50\Omega$  are connected to ports 1, 2 and 3.



**Figure 2.** The ideal circuit of the wideband balun bandpass filter.

The simulated frequency responses (simulated with Ansoft Designer v3.0) of Fig. 2 with/without the coupled lines are shown in Fig. 3. Obviously, DC suppression and in-band balance improvement can be achieved by the introduction of the open coupled lines. In addition, a transmission zero is produced by the open coupled lines for the second harmonic suppression of  $|S_{21}|$  &  $|S_{31}|$ . To better investigate the transmission characteristic of the proposed balun filter, the differential mode equivalent circuit of



**Figure 3.** Simulated frequency responses of Fig. 2. ( $Z_{oe} = 163.1 \Omega$ ,  $Z_{oo} = 86.5 \Omega$ ,  $Z_1 = 12 \Omega$ ,  $Z_2 = 120 \Omega$ ,  $Z_s = 124 \Omega$ ,  $\theta = 90^\circ$ ).

the balanced circuit in Fig. 2 is shown as Fig. 4(a), when the even-mode is excited. A virtual open appears along the plane  $A - A'$  (as shown in Fig. 4(b)), and the even-mode input admittance  $Y_{ine}$  of Fig. 4(b) is

$$Y_{ine} = j \frac{Z_1 \tan \theta - (Z_1 Z_2 / 2Z_3 + Z_2 + Z_2^2 / 2Z_3) \cot \theta}{Z_1 Z_2 + Z_1 Z_2^2 / 2Z_3} \quad (5)$$

When  $Y_{ine} = 0$ , two resonator frequencies for the even-mode can be acquired

$$\begin{aligned} \theta_{even1} &= \arctan \sqrt{Z_2 / 2Z_3 + Z_2 / Z_1 + Z_2^2 / 2Z_1 Z_3} \\ \theta_{even1} &= \pi - \arctan \sqrt{Z_2 / 2Z_3 + Z_2 / Z_1 + Z_2^2 / 2Z_1 Z_3} \end{aligned} \quad (6)$$

For the odd-mode excitation, a virtual short appears along the plane  $A - A'$  (as shown in Fig. 4(c)), and the odd-mode input admittance  $Y_{ino}$  of Fig. 3(c) is

$$Y_{ino} = -j(Z_1 + Z_2) \cot \theta / Z_1 Z_2 \quad (7)$$

When  $\theta = 90^\circ$ ,  $Y_{ino}$  equals to zero, and another resonant frequency occurs at the center frequency  $f_0$  for the symmetrical balanced circuit.

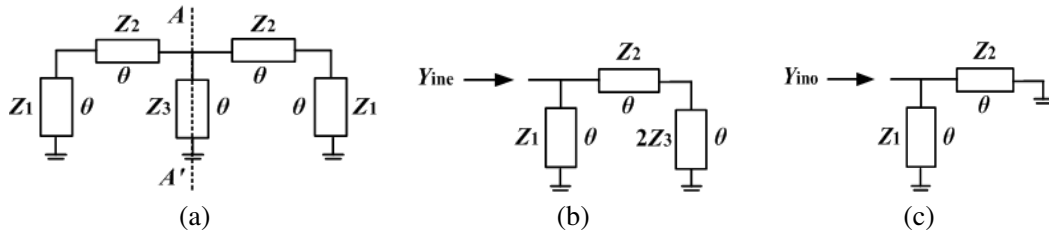


**Figure 4.** (a) Differential mode circuit of the balanced structure in Fig. 2; (b) Even-mode equivalent circuit; (c) Odd-mode equivalent circuit.

Figures 5(a)–(d) plot the even/odd-mode resonant frequencies versus  $\theta$  and characteristic impedance  $Z_1$ ,  $Z_2$  and  $Z_3$  (under weak coupling).  $f_0$  is the center frequency of the balun bandpass filter, and the bandwidth of the balun filter is mainly determined by the even-modes  $f_{even1}$  and  $f_{even2}$ . In addition, the even-modes  $f_{even1}$  and  $f_{even2}$  move away from  $f_0$  as  $Z_1$ ,  $Z_3$  increase but towards  $f_0$  as  $Z_2$  increases. To realize a wide passband for the balun filter, when  $Z_{oe}$ ,  $Z_{oo}$  and  $\theta$  are determined, we can adjust the characteristic impedance  $Z_1$ ,  $Z_2$  and  $Z_3$  to determine the even-modes  $f_{even1}$  and  $f_{even2}$  frequencies, and the needed bandwidth for the balun filter can be achieved.

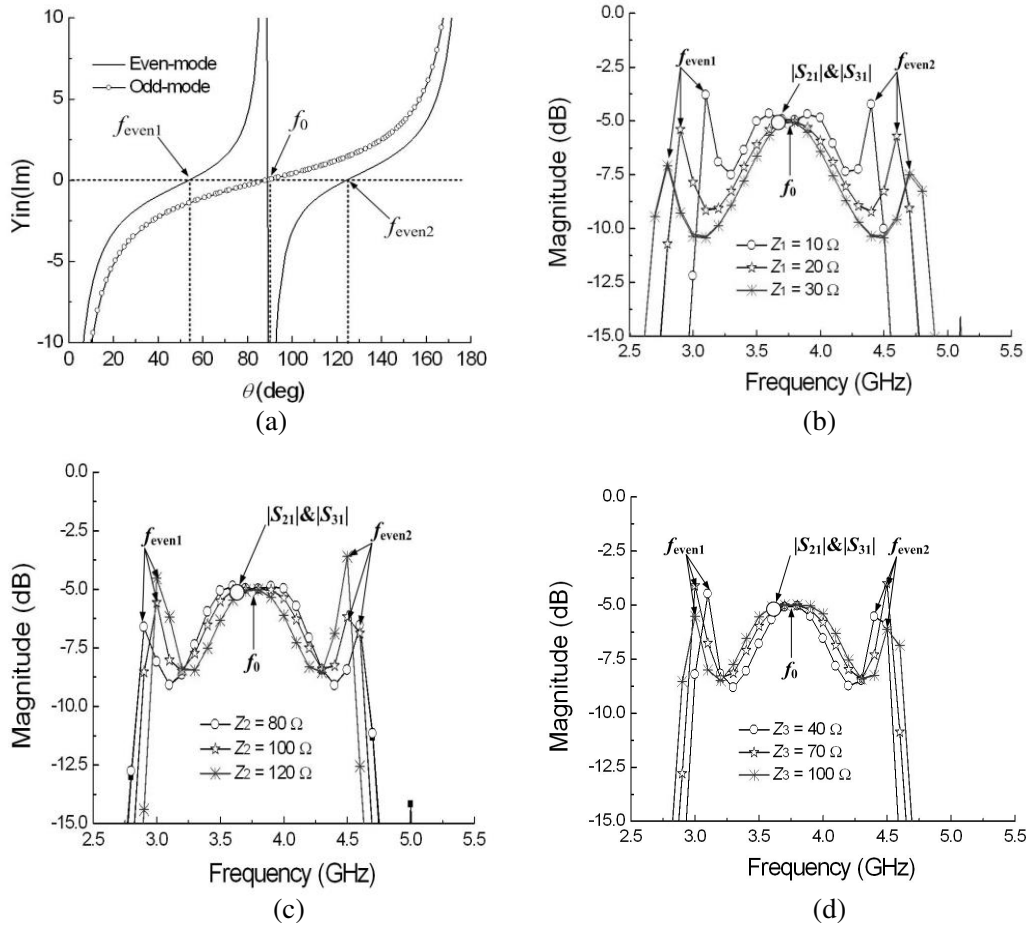


**Figure 5.** (a) Analysis of resonator frequencies versus  $\theta$  ( $Z_2/Z_1 = Z_3/Z_1 = 1$ ); (b)  $|S_{21}|$  &  $|S_{31}|$  versus  $Z_1$ ,  $Z_2 = 100 \Omega$ ,  $Z_3 = 100 \Omega$ ; (c)  $|S_{21}|$  &  $|S_{31}|$  versus  $Z_2$ ,  $Z_1 = 15 \Omega$ ,  $Z_3 = 100 \Omega$ ; (d)  $|S_{21}|$  &  $|S_{31}|$  versus  $Z_3$ ,  $Z_1 = 15 \Omega$ ,  $Z_3 = 100 \Omega$  ( $Z_{oe} = 144.5 \Omega$ ,  $Z_{oo} = 108.5 \Omega$ ).

Based on the above filter analysis, the design procedures of the wideband balun bandpass filter can be summarized as follows:

- (1) Choose the desired center frequency  $f_0$  of the balun bandpass filter and determine the coupling coefficient  $k$  ( $k = (Z_{oe} - Z_{oo}) / (Z_{oe} + Z_{oo})$ ), line width  $W$  and gap size  $g$  of the coupled lines;
- (2) Adjust the characteristic impedances  $Z_s$ ,  $Z_1$  and  $Z_2$ , obtain the desired 3-dB bandwidth for the balun filter, maximize the commonmode resonance suppression, and optimize the in-band balance for the balun bandpass filter.

The final parameters for the filter circuit of Fig. 2 are:  $Z_0 = 50 \Omega$ ,  $Z_1 = 12 \Omega$ ,  $Z_2 = 120 \Omega$ ,  $Z_s = 124 \Omega$ ,  $Z_{oe} = 163.5 \Omega$ ,  $Z_{oo} = 88.1 \Omega$ ,  $f_0 = 3.75$  GHz. The structure parameters for the balun filter (with size of  $45 \text{ mm} \times 43 \text{ mm}$  or  $0.82\lambda_g \times 0.78\lambda_g$ ) in Fig. 6 are:  $W = 0.2 \text{ mm}$ ,  $W_0 = 1.37 \text{ mm}$ ,  $W_1 = 8.7 \text{ mm}$ ,  $W_2 = 0.24 \text{ mm}$ ,  $W_s = 0.2 \text{ mm}$ ,  $l_1 = 24.8 \text{ mm}$ ,  $l_2 = 9.24 \text{ mm}$ ,  $l_3 = 1.31 \text{ mm}$ ,  $l_4 = 3.92 \text{ mm}$ ,  $l_5 = 2.62 \text{ mm}$ ,  $m_1 = 3.45 \text{ mm}$ ,  $m_2 = 3.9 \text{ mm}$ ,  $m_3 = 4.0 \text{ mm}$ ,  $m_4 = 2.42 \text{ mm}$ ,  $m_5 = 2.0 \text{ mm}$ ,  $n_1 = 7.44 \text{ mm}$ ,  $n_2 = 7.7 \text{ mm}$ ,  $n_3 = 6.84 \text{ mm}$ ,  $tl_1 = 0.4 \text{ mm}$ ,  $tl_2 = 4.07 \text{ mm}$ ,  $g = 0.23 \text{ mm}$ . The simulated results with Ansoft Designer v3.0 and Ansoft HFSS v.11.0 are shown in Fig. 7. Good agreement can be found between the simulated results. The simulated 3-dB fractional bandwidth is 34.7% (3.1–4.4 GHz). The minimum insertion loss is 3.7 dB in each path. A three-order passband with return loss greater than 12.5 dB is realized for the balun bandpass filter, and over 20 dB upper stopband is obtained from 5 to 10 GHz ( $2.67f_0$ ). In addition, the amplitude and phase imbalances in the passband of the balun bandpass filter are less than 0.18 dB and  $0.3^\circ$ , respectively.

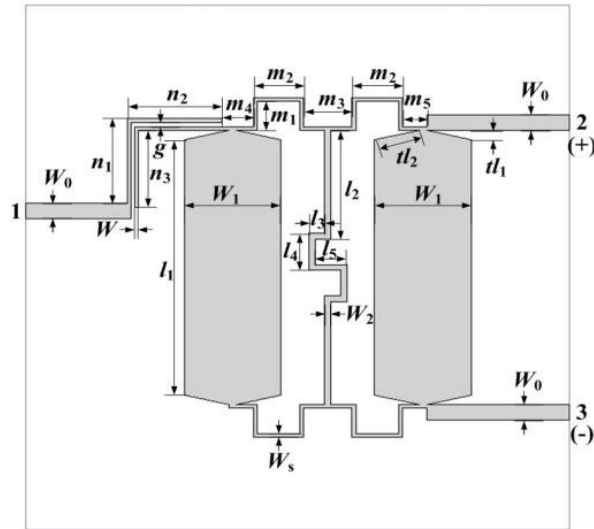


Figure 6. Top view of proposed wideband balun bandpass filter.

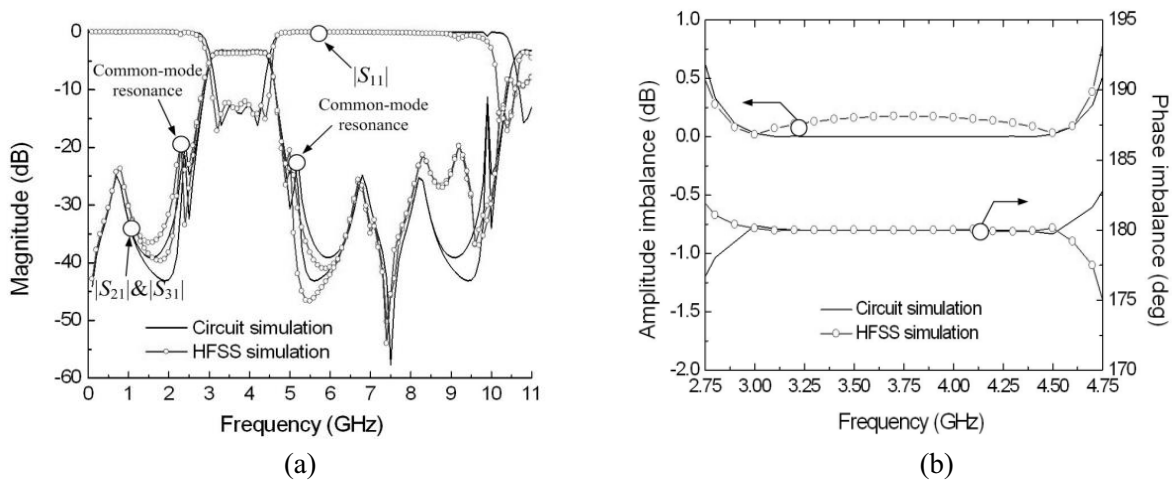
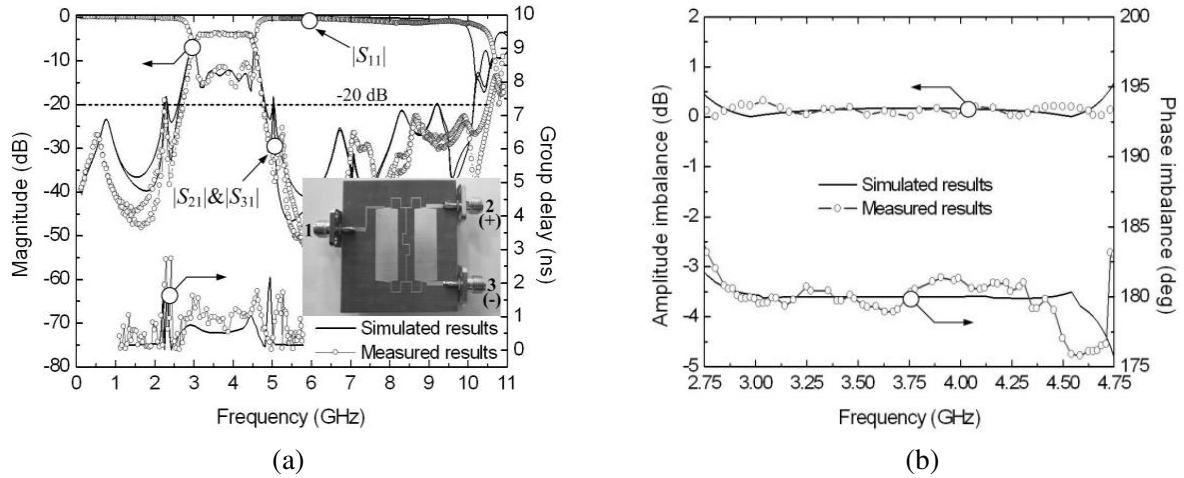


Figure 7. Simulated results for the balun bandpass filter. (a) Frequency responses; (b) Amplitude and phase imbalances.

### 3. MEASURED RESULTS AND DISCUSSIONS

For demonstration, a wideband balun bandpass filter with center frequency 3.75 GHz is designed and fabricated. Fig. 8 shows a photograph of the proposed wideband balun bandpass filter with size of 45 mm × 43 mm (0.82λ<sub>g</sub> × 0.78λ<sub>g</sub>), which is fabricated on the substrate with ε<sub>r</sub> = 2.65, h = 0.5 mm, and tan δ = 0.003. The measured results for the wideband balun bandpass filter are also shown in Figs. 8(a) and (b). The measured 3-dB fractional bandwidth is 33.8% (3.13–4.4 GHz). The minimum insertion loss is 4.35 dB in each path. The return loss is greater than 10 dB in the passband. Over 20 dB upper stopband is obtained from 5 to 10.5 GHz (2.8f<sub>0</sub>), and the group delay is less than 1.2 ns in the pass band.

In addition, the amplitude and phase imbalances in the passband of the balun bandpass filter are less than 0.25 dB and 1.3°, respectively. The slight frequency discrepancies between the measured and simulated results are mainly caused by the fabrication precision limitation and measurement errors. Moreover, due to the low characteristic impedance of the stub (Z<sub>1</sub>, 2θ), some mismatching errors exist



**Figure 8.** Measured and simulated results for the balun bandpass filter. (a) Frequency responses; (b) Amplitude and phase imbalances.

in the wideband balun structure. Two shunt-connected transmission lines for the transmission line with characteristic impedance  $2Z_1$  and electrical length  $2\theta$  can be used to reduce the practical mismatching error.

#### 4. CONCLUSION

A novel wideband balun bandpass filter is proposed based on a four-port balanced circuit with one port opened. A pair of open coupled lines is used to realize DC suppression and balun in-band balance improvement. The proposed wideband balun bandpass filter shows advantages of controllable fractional bandwidth, high selectivity, excellent in-band balance performances and extended stopband, indicating a good candidate for wideband wireless applications.

#### ACKNOWLEDGMENT

This work is supported by the National Natural Science Foundation of China (61401206), Natural Science Foundation of Jiangsu Province (BK2014 0791) and the 2014 Zijin Intelligent Program of Nanjing University of Science and Technology.

#### REFERENCES

1. Jung, E.-Y. and H.-Y. Hwang, "A balun-BPF using a dual mode ring resonator," *IEEE Microw. Wireless Compon. Lett.*, Vol. 17, 652–654, 2007.
2. Wu, S. M., C. T. Kuo, and C. H. Chen, "Very compact full differ-ential bandpass filter with transformer integrated using integrated passive device technology," *Progress In Electromagnetics Research Letters*, Vol. 113, 251–267, 2001.
3. Ang, K. S., Y. C. Leong, and C. H. Lee, "Analysis and design of miniaturized lumped-distributed impedance-transforming baluns," *IEEE Trans. Microw. Theory Techn.*, Vol. 51, 1009–1017, 2003.
4. Ang, K. S. and I. D. Robertson, "Analysis and design of impedance-transforming planar Marchand baluns," *IEEE Trans. Microw. Theory Techn.*, Vol. 49, 402–406, 2001.
5. Zhang, Z.-Y., Y.-X. Guo, L. C. Ong, and M. Y. W. Chia, "A new wide-band planar balun on a single-layer PCB," *IEEE Microw. Wireless Compon. Lett.*, Vol. 15, 416–418, 2005.
6. Wu, C. H., C. H. Wang, S. Y. Chen, and C. H. Chen, "Balanced-to unbalanced bandpass filters and the antenna application," *IEEE Trans. Microw. Theory Techn.*, Vol. 56, 2474–2482, 2008.

7. Yang, T., M. Tamura, and T. Itoh, "Compact hybrid resonator with series and shunt resonances used in miniaturized filters and balun filters," *IEEE Trans. Microw. Theory Techn.*, Vol. 58, 390–402, 2010.
8. Xue, Q., J. Shi, and J. X. Chen, "Unbalanced-to-balanced and balanced-to-unbalanced diplexer with high selectivity and common-mode suppression," *IEEE Trans. Microw. Theory Techn.*, Vol. 58, 970–977, 2010.
9. Eisenstant, W. R., B. Stengel, and B. M. Thompson, *Microwave Differential Circuit Design Using Mixed-mode S-parameters*, Artech House, Boston, MA, 2006.
10. Leong, Y. C., K. S. Ang, and C. H. Lee, "A derivation of a class of 3-port baluns form symmetrical 4-port networks," *IEEE MTT-S Int. Microw. Symp. Dig.*, 1165–1168, 2002.
11. Wang, H., W. Kang, G. Yang, and W. Wu, "A wideband differential bandpass filter based on T-shaped stubs and single ring resonator," *Progress In Electromagnetic Research Letter*, Vol. 40, 39–48, 2013.
12. Feng, W. J., W. Q. Che, L. M. Gu, and Q. Xue, "High selectivity wideband balanced bandpass filters using symmetrical multi-mode resonators," *IET Microw. Antennas Propag.*, Vol. 7, 1005–1015, 2013.